TITLE PAGE

Durable pharmacological responses from the peptide ShK-186, a specific Kv1.3 channel inhibitor that suppresses T cell mediators of autoimmune disease.

Eric J. Tarcha, Victor Chi, Ernesto J. Muñoz-Elías, David Bailey, Luz M. Londono, Sanjeev K. Upadhyay, Kayla Norton, Amy Banks, Indra Tjong, Hai Nguyen, Xueyou Hu, Greg W. Ruppert, Scott E. Boley, Richard Slauter, James Sams, Brian Knapp, Dustin Kentala, Zachary Hansen, Michael W. Pennington, Christine Beeton, K. George Chandy, and Shawn P. Iadonato

Kineta Inc., 219 Terry Ave N, Suite 300, Seattle, WA 98109-5208 (E.J.T, E.J.M., L.L., A.B., K.N., S.P.I.), Department of Physiology and Biophysics and the Department of Surgery, UC Irvine, Irvine, CA 92697 (V.C., S.K.U., K.G.C.), MPI Research, 54943 North Main Street, Mattawan, MI 49071-9399 (G.W.R., S.E.B., R.S., J.S., B.K., D.K., Z.H.), Peptides International, 11621 Electron Drive, Louisville, KY 40299 (M.W.P.), and Department of Molecular Physiology and Biophysics, Baylor College of Medicine, Houston, TX 77030 (X.H., C.B.)

RUNNING TITLE PAGE

a) Durable pharmacological responses from ShK-186

b) Corresponding author: Eric J. Tarcha, 219 Terry Ave N., Suite 300, Seattle, WA 98109-5208;

Tel: 206-378-0400; Fax: 206-378-0408; Email: eric@kineta.us

c) Text pages: 27

Tables: 2

Figures: 6

References: 39

Abstract: 242

Introduction: 815

Discussion: 1162

d) Abbreviations: ACN, acetonitrile; ADME, absorption, distribution, metabolism, excretion; ANOVA, analysis of variance; AT-EAE, adoptive transfer experimental autoimmune encephalomyelitis; AUC_{0-inf}, area under the concentration-time curve from 0 to infinity; CFA, complete Freund's adjuvant; C_{max}, maximum plasma concentration; CT, computed tomography; DA, Dark Agouti; DMF, dimethylformamide; DOTA, 1,4,7,10-tetraazacyclododecane-1,4,7,10-tetraacetic acid; DTH, delayed-type hypersensitivity reaction; CR-EAE, chronic-relapsing experimental autoimmune encephalomyelitis; EDTA, ethylene diamine tetraacetic acide; ELISA, enzyme-linked immunosorbent assay; Fmoc, Fluorenylmethyloxycarbonyl; HOBt, N-Hydroxybenzotriazole; HPLC, high pressure liquid chromatography; IACUC, institutional animal care and use committee; LOQ, limit of quantitation; MS, mass spectrometry; OVA, ovalbumin; PBMC, peripheral blood mononuclear cell; PD, pharmacodynamic; PIA, pristane-induced arthritis; PK, pharmacokinetic; POC, Percent of Control; RA, rheumatoid arthritis; SD, Sprague

Dawley; SPECT, single-photon emission computed tomography; t-bu, tertiary butyl; TCA,

trichloroacetic acid; TFA, trifluoroacetic acid

<u>e) Drug Discovery and Translational Medicine</u>

ABSTRACT

The Kv1.3 channel is a recognized target for pharmaceutical development to treat autoimmune diseases and organ rejection. ShK-186, a specific peptide inhibitor of Kv1.3, has shown promise in animal models of multiple sclerosis and rheumatoid arthritis. Here, we describe the pharmacokinetic - pharmacodynamic relationship for ShK-186 in rats and monkeys. The pharmacokinetic profile of ShK-186 was evaluated with a validated HPLC-MS/MS method to measure the peptide's concentration in plasma. These results were compared with SPECT/CT data collected with an ^{111}In-DOTA-conjugate of ShK-186 to assess whole blood pharmacokinetic parameters as well as the peptide's absorption, distribution and excretion. Analysis of these data support a model wherein ShK-186 is absorbed slowly from the injection site resulting in blood concentrations above the Kv1.3 channel-blocking IC_{50} value for up to 7 days in monkey. Pharmacodynamic studies on human peripheral blood mononuclear cells showed that brief exposure to ShK-186 resulted in sustained suppression of cytokine responses and may contribute to prolonged drug effects. In delayed-type hypersensitivity, chronic relapsing-remitting experimental autoimmune encephalomyelitis and pristane-induced arthritis rat models, a single dose of ShK-186 every 2 – 5 days was as effective as daily administration. ShK-186's slow distribution from the injection site and its long residence time on the Kv1.3 channel contribute to the prolonged therapeutic effect of ShK-186 in animal models of autoimmune disease.

INTRODUCTION

The Kv1.3 channel has been an active target of pharmaceutical development for more than 15 years (recently reviewed in Chi et al., 2011). The interest in this channel derives from its important function in activated effector-memory (T_{EM}) T cells, which are major mediators of autoimmune disease (Beeton et al., 2006; Wulff et al., 2003). Engagement of the T cell receptor by antigen presenting cells results in an influx of calcium into the cytoplasm, initially from the endoplasmic reticulum but subsequently from the extracellular space via the CRAC channel (reviewed in Cahalan and Chandy 2009). The opening of voltage-gated Kv1.3 and calcium-activated KCa3.1 potassium channels in the T cell membrane and the resulting efflux of potassium ions promotes calcium entry and sustains intracellular calcium at concentrations necessary for T cell activation (reviewed in Cahalan and Chandy 2009). Resting T cells express a mixture of both K^+ channels. However, upon activation, naïve and central-memory T (T_{CM}) cells increase expression of the KCa3.1 channel, while T_{EM} cells upregulate Kv1.3 channel expression (Wulff et al., 2003). In the latter cell population, the degree of Kv1.3 expression is a measure of cell activation, and the channel is required for the maintenance of the T_{EM} cell-phenotype (Hu et al., 2007; Hu et al., 2012).

We and others have previously shown that Kv1.3^{HIGH} CCR7$^-$ activated T_{EM} cells are present at sites of inflammation in autoimmune disease, and auto-reactive T cells from subjects with multiple sclerosis, type 1 diabetes, and rheumatoid arthritis express the Kv1.3^{HIGH} phenotype of activated T_{EM} cells (Rus et al., 2005; Beeton et al., 2006). In addition, specific Kv1.3-inhibitors have been found to be effective in numerous animal models of inflammation including adoptive and chronic relapse-remitting experimental autoimmune encephalomyelitis (AT-EAE, CR-EAE) (Beeton et al., 2005; Beeton et al., 2006), pristane-induced arthritis (PIA) (Beeton et al., 2006), the delayed-type hypersensitivity (DTH) reaction (Koo et al., 1997; Beeton et al., 2005; Matheu et al., 2008), allergic contact dermatitis (Azam et al., 2007), allogeneic kidney transplant (Grgic

et al., 2009), spontaneous autoimmune diabetes (Beeton et al., 2006), vascular neointima hyperplasia (Choeng et al., 2011), anti-glomerular basement membrane glomerulonephritis (Hyodo et al., 2010), and psoriasis (Gilhar et al., 2010). For these reasons, numerous groups have focused on developing specific and potent inhibitors of the Kv1.3 channel for the treatment of inflammation and autoimmune disease (reviewed in Cahalan and Chandy 2009, Rangaraju et al., 2009). Much of this effort has focused on developing small molecule inhibitors of Kv1.3, but identifying compounds that are adequately specific has proved challenging, and to date, no drug specifically targeting Kv1.3 has entered clinical trials.

Our group is developing ShK-186, a 37-amino acid selective peptide inhibitor of Kv1.3, as a therapeutic for autoimmune diseases. To date, the FDA has approved more than 55 peptide drugs in roughly 33 mechanistic classes, making peptides one of the most active areas of biologics drug research. However, the peptide field has suffered from a perception that frequent dosing is required for sustained pharmacodynamic (PD) activity and that patients have a poor acceptance of parenteral therapies. Therefore, careful attention to dose frequency and dose presentation are important to the development of a commercially viable peptide drug. Here, we report on the optimization of ShK-186 dose and dose frequency in animal models of autoimmune disease as part of our recently completed nonclinical program for the peptide.

Previous studies from our group have characterized the level of Kv1.3 channel-blocking activity in the serum of Lewis rats following single subcutaneous injections of three related analogs ShK(L5), ShK-186 and ShK-192 (Beeton et al., 2005, Matheu et al., 2009, Pennington et al., 2009). Peak serum drug activity occurred 30 min following injection and returned to baseline by 7 h post-dose, but ~200 pM concentration of functionally active peptide was detected in the blood 24 and 48 h after injection, and approximately 100 pM was detectable at 72 h (Beeton et al., 2005, Matheu et al., 2009, Pennington et al., 2009). However, previous animal studies that investigated ShK peptides were performed using a once-daily or greater than once-daily dosing

frequency (Beeton et al., 2001, Beeton et al., 2005, Beeton et al., 2006, Matheu et al., 2008, Pennington et al., 2009). Here, we demonstrate that ShK-186 has a long-lasting therapeutic effect in three different rat models of autoimmune disease due to its slow release from the site of subcutaneous injection and its tight binding to and slow-release from the Kv1.3 channel on T cells.

METHODS

Animals. DA and Lewis rats, 8-10 weeks old, were purchased from Harlan Laboratories (Indianapolis, IN, USA) and housed under pathogen-free conditions with food and water *ad libitum*. DTH trials were approved by the Baylor College of Medicine and Infectious Disease Research Institute (IDRI) Institutional Animal Use and Care Committees (IACUC). EAE trials were approved by the University of California at Irvine and the IDRI IACUCs. PIA trials were approved by the Baylor College of Medicine IACUC.

Sprague Dawley [Crl:CD®SD] rats (6 – 9 weeks old) were purchased from Charles River Laboratories (Willmington, MA, USA) and housed in a temperature (64^0C-79°C) and humidity (30-70%) controlled facility. Food and water were *ad libitum*. PK studies in SD rats were approved by either the MPI Research or IDRI IACUCs.

Non-naïve cynomolgus (*Macaca fascicularis*) and squirrel monkeys (*Saimiri boliviensis*) were between 2 and 5 years of age and were transferred from the MPI Research (Mattawan, MI, USA) stock colony. All cynomolgus monkeys were of Chinese origin. The squirrel monkey was of Bolivian origin and obtained originally from the University of Texas MD Anderson Cancer Center (Houston, TX USA). Animals were housed individually in stainless steel cages in an environmentally controlled room. The monkeys were provided environmental enrichment; fluorescent lighting was provided 12 h / day. Temperature was maintained between 64^oC and 84°C; humidity was 30-70%. Animals were provided Certified Primate Diet (PMI Nutrition International, Inc., St. Louis, MO, USA) twice daily. Primatreats® and other enrichment foods were provided on a regular basis. Water was available *ad libitum*. Primate studies were approved by the MPI Research IACUC.

Kv1.3 peptide inhibitors. ShK-186 and ShK-198 (derivatives of ShK [Accession: P29187]) were manufactured using an Fmoc-tBu solid-phase strategy on an amide resin. All of the coupling steps were mediated with 6-Cl-HOBT in the presence of diisopropyl carbodiimide.

Fmoc removal was facilitated with 20% piperidine in DMF containing 0.1 M HOBt to buffer the piperidine and minimize potential racemization at the 6 Cys residues. Following assembly, the peptide was cleaved from the resin and simultaneously deprotected using a TFA cleavage cocktail (Reagent K) containing aromatic cationic scavengers for 2 h at RT. The crude peptide was filtered from the spent resin and subsequently isolated by precipitation into ice cold diethyl ether. The crude peptide was dissolved in 50% acetic acid and subsequently diluted into 3 L of H_2O. The pH of this peptide solution was adjusted to 8.0 with NH_4OH and allowed to slowly stir overnight. Disulfide bond formation was mediated by air oxidation or through the addition of a glutathione exchange system. ShK and its derivatives spontaneously fold to a major thermodynamically favored isomer which is the biologically active form of the peptides. The folded peptide was loaded onto a preparative RP-HPLC column and purified using a gradient of ACN versus H_2O containing 0.05% TFA. The fractions containing the desired peptide purity were pooled together and lyophilized to produce an acetate salt. Drug was formulated at 0.5 – 25 mg/mL in 10mM sodium phosphate, 0.8% NaCl, 0.05% polysorbate 20, pH 6.0.

Serum and plasma stability studies. Shk-186 peptide was solubilized at a concentration of 10 mg/mL in formulation buffer. 25 µl of the stock peptide solution was spiked into 475 µl of a 1:1 dilution of serum, plasma, or whole blood with RPMI to a final concentration of 0.5 mg/ml and incubated at 37°C for the indicated period. 50 µl of the sample was then mixed with 50 µl 4% trichloro-acetic acid (TCA), and the sample was vortexed for 30 sec and placed at 4°C for 15 min. The TCA mixture was centrifuged at 12,000 RPM for 5 min to pellet the precipitated proteins, and the supernatant was analyzed on an Agilent 1100 HPLC system fitted with a Grace Vydac C18, 5.0 µm, 300 Å, 4.6 x 250 mm column (Grace, Deerfield, IL, USA). Mobile phase A was composed of 0.1%TFA in 95% water/5% ACN, and mobile phase B was composed of 0.1% TFA in 5% Water/95% ACN. The system flow rate was 1 mL/min.

HPLC-MS/MS method for measuring ShK-186 and metabolites in plasma. Whole-blood samples were collected into K_2EDTA-containing tubes and processed by centrifugation to plasma. Plasma was supplemented 20:1 (v/v) with HALT® Phosphatase Inhibitor Cocktail (Thermo Scientific, Rockford IL, USA) and stored frozen at -70°C until analysis. 50 µL of an internal standard [2 µg/mL ShK (parent peptide, Accession number: P29187)] in 90:10 H_2O:ACN v/v; Bachem AG, Bubendorf, Switzerland) were added to 100 µL of plasma. The combined sample was diluted with 300 µL H_2O and purified using a Waters Sep-Pak® tC18, 25mg, 96-well SPE plate (Millford, MA, USA). Samples were eluted in 500 µL TFA/H_2O/ACN (1:70:30, v/v) and evaporated under N_2. The residue was reconstituted in 200 µL TFA/H_2O/ACN (0.02:90:10, v/v/v) and analyzed by HPLC-MS/MS. HPLC was performed on an Agilent 1200 series instrument fitted with an ACE 5 C18-PFP 50 x 2.1 mm, 5 µm column (Advanced Chromatography Technologies, Aberdeen, UK). Mobile phase A was formic Acid/H_2O (2:1000, v/v), and mobile phase B was formic acid/H_2O/ACN (2:500:500, v/v/v). The flow rate was 300 µL/min. Mass spectrometry was performed on a SCIEX API 5000 instrument (AB Sciex, Foster City, CA, USA) using turbo ion spray in the positive mode. Mass detection was performed using multiple reaction monitoring (ShK-186 m/z 741.5→841.0, ShK-198 m/z 728→840.6, internal standard m/z 676.8→769.0). The dwell times for the internal standard, ShK-186, and ShK-198 were each 500 ms.

SPECT/CT scanning of radiolabeled ShK-221. ShK-221 (100 µg) was radiolabelled with 2 mCi [111]Indium chloride (GE Healthcare, Arlington Heights, IL USA) in a 300 µL reaction containing 50 mM sodium acetate, pH 5.0 for 30 min at 95°C. The reaction was quenched by the addition of EDTA to a final concentration of 50 mM, and the radiolabeling efficiency was assessed by reverse-phase HPLC (Luna 5µ C18(2) 100A 250 x 4.6 mm column, Phenomenex, Torrance, CA USA) on an Agilent 1100 system using an IN/US Systems Gamma RAM Model 4 radio-HPLC detector (LabLogic Systems, Brandon, FL USA). The labeling efficiency varied from

89-98% by this method. SPECT/CT scanning (NanoSPECT/CT Preclinical Imager, Mediso, Budapest, Hungary) was carried out on anesthetized animals in four 15 min scans during the first hour and one scan each at 4, 8, 24, 48, 72, 120 and 160 h post-dose. The individual projection frame time for each helical SPECT was set such that the duration of each scan would last for approximately 15 to 45 min (varying by time-point to account for isotope decay) and allow for significant collection of statistics within each frame. The characteristic peaks detected from the spectra for ^{111}In were 245 and 171 keV (primary and secondary, respectively). The resulting projection data were reconstructed after each scan using an iterative model that takes advantage of the pinhole geometry to achieve a resolution of approximately 2 mm.

Approximately 10 µL blood samples were collected after each scan and the amount of radioactivity in the sample was measured using a Wallac Wizard 1470 scintillation counter (Perkin Elmer, Waltham, MA USA). Drug concentrations were computed by taking account of the specific activity of the administered dose, the half-life of ^{111}In (67.3 h) and the counting efficiency of the instrument.

Suppression of cytokine responses in peripheral blood mononuclear cells (PBMCs). PBMCs were isolated from human whole blood using CPT® Vacutainers (Beckton, Dickinson, Franklin Lakes, New Jersey, USA) and dispersed into RPMI media. 100 µL of media containing 2×10^5 PBMCs were added to each well of a 96-well dish and treated with the addition of 50 µL ShK-186 in media at varying concentrations for 1 h at 37°C, 5% CO_2. Cells were washed twice with RPMI, resuspended in 200 µL fresh media supplemented with 40 µM thapsigargin, and stimulated for 48 h at 37°C, 5% CO_2. Cytokine production was measured in the overlying media using a Luminex Assay (Millipore, Bellerica, MA, USA) specific for IL-2.

DTH model in rat. Active DTH was induced and monitored as described (Beeton and Chandy 2007). Briefly, Lewis rats were immunized in the flanks with ovalbumin (OVA) (200 µg/rat) emulsified in complete Freund's adjuvant (CFA) (Sigma, St Louis, MO, USA). Seven to nine

days later, animals were challenged under isoflurane anesthesia in the pinna of one ear with 20 µg OVA dissolved in saline and in the other ear with saline. Animals received one or two subcutaneous injection(s) of either ShK-186 or vehicle at the time of challenge or on the four days preceding challenge. Thickness of both ears was measured 24 h after challenge with a spring-loaded micrometer (Mitutoyo America Corporation, Aurora, IL, USA).

CR-EAE model in rat. The CR-EAE model in DA rats (Lorentzen et al., 1995) was used with minor modifications. Briefly, animals were immunized by subcutaneous injection at the base of the tail with 0.2 ml of a 1:1 emulsion of homogenized SD rat spinal cord (Bioreclamation LLC) in CFA supplemented to 4 mg/ml of *M. tuberculosis* H37Ra (Sigma, St Louis, MO, USA) under isoflurane anesthesia. Each rat received ~80 mg of spinal cord and 400 µg of H37Ra. Either ShK-186 or placebo was administered subcutaneously on alternate flanks as appropriate. Animals were observed daily by measuring their body weight and assessing clinical signs of disease. Animals were included in the study and randomized into experimental groups sequentially as they reached a clinical score of 1. Scores were assigned as follows: 0, no illness; 0.5, no tail coil; 1, no tail coil and flaccid tail (tail dropped straight down 5 consecutive times); 2 mild paraparesis, wobbling; 3, moderate to severe paraparesis, falling on its side, unable to stand on hind legs; 3.5, 1 limb paralysis; 4, 2 limb paralysis; 5, 2 limb paralysis with incontinence; 6, death. A cumulative clinical score was calculated for each rat by adding the daily scores from the day of disease onset (CS =>1) until the end of treatment and averaged to obtain a mean cumulative clinical score. Disease prevalence was calculated as the number of animals with CS > 0.5 divided by the number of living animals per day and expressed as a percentage. During the chronic phase, an animal was considered to have a relapse if its clinical score was greater than 1.

Pristane-induced arthritis in rats. Female DA rats received 150 µl pristane (2, 6, 10, 14-tetramethylpentadecane, CosmoBio, Carlsbad, CA) by subcutaneous injection in two sites at the

base of the tail under isoflurane anesthesia. ShK-186 or vehicle was administered subcutaneously in the scruff of the neck daily or every other day for the duration of the trial. All four limbs were monitored for arthritis as described (Rintish et al, 2009). Briefly, a score of 1 point was given for each swollen and red toe, and each mid-foot, digit, or knuckle, and 5 points for each swollen ankle or wrist (maximum score per limb 15; maximum score per animal 60). All these studies were done under an IACUC approved protocol at Baylor College of Medicine.

Statistical and computational analysis. Statistical analysis was carried out using the one-way ANOVA (EAE model and cytokine expression studies), the two-tailed, Mann-Whitney U test (DTH model) or the paired t-test (pharmacokinetic studies). Goodness of model fit was determined using the R^2 statistic. Pharmacokinetic calculations were as follows: C_{max} and T_{max} were as observed in the dataset. AUC was computed using a linear trapezoidal method. The terminal elimination half-life was computed from the slope of the regression with the best adjusted R^2 value. $AUC_{t-\infty}$ was calculated by dividing the last observed drug concentration by the terminal elimination slope.

RESULTS

Pharmacokinetic properties of ShK-186 in representative species. As a precursor to PK studies of ShK-186 in nonclinical species, we evaluated the stability of the peptide in serum, plasma, and whole blood from human, Sprague Dawley rat and cynomolgus monkey (*Macaca fascicularis*). Spiking-in studies showed the formation of a single metabolite in all samples analyzed from all three species. The metabolite was characterized by mass spectrometry and shown to be the dephosphorylated form of ShK-186 (referred to as ShK-198, Suppl. Fig. 1A-C). ShK-198 is identical to the previously described analog ShK(L4) with the exception of containing a C-terminal amide in place of a carboxyl (Beeton et al., 2005). ShK(L4) blocks Kv1.3 with an IC_{50} of 48 pM (Beeton et al., 2005), which is similar to the potency of ShK-198 (Fig. 2A and 2C; IC_{50} = 41.4 ± 7.25 pM, n = 5). Conversion of ShK-186 to ShK-198 occurred most readily in serum and in plasma samples treated with citrate or heparin as the anticoagulant. ShK-186 is most stable in plasma containing K_2EDTA or specific phosphatase inhibitors (sodium fluoride, sodium orthovanadate, sodium pyrophosphate and beta-glycerophosphate), suggesting that endogenous phosphatases are responsible for its conversion.

We developed and validated an HPLC-MS/MS method to measure concentrations of ShK-186 and ShK-198 in K_2EDTA plasma of rats and cynomolgus monkeys. The method had a lower limit of quantitation (LOQ) of 2 ng/mL (~450 pM) for each analyte. The method showed equivalent recovery of ShK-186 from both spiked plasma and spiked buffer QC samples. Using this method, we measured the *in vivo* pharmacokinetic properties of ShK-186 following a single subcutaneous administration (the intended clinical route of administration) to rat and monkey. Both rat and monkey have T_{EM} cells that express large numbers of the Kv1.3 channel after activation and are therefore relevant nonclinical species for testing ShK-186 (Chi et al., 2011).

The PK profile of ShK-186 is characterized by a short residence time in the central compartment of rat and monkey species. In rat, following a single administration, ShK-186 reaches a

maximum plasma concentration between 1 and 5 min, whereas its metabolite reaches its C_{max} between 1 and 15 min (Fig. 1A and B and Table 1 and 2). While the C_{max} and AUC for both the parent and metabolite increase with dose in rat, the relationship between C_{max} and dose was largely non-linear (R^2=0.8), whereas the relationship between AUC and dose was roughly linear through the 500 µg/kg dose (R^2=0.97, Fig. 1E). The half-life in rat ranged from 4.4 to 9.2 min for ShK-186 and from 6.1 to 16.4 min for ShK-198 (Table 1 and 2). Clearance values for ShK-186 and ShK-198 in rat were not significantly different (paired t-test, t(4)=2.2, p=0.1) and ranged from 441.4 to 1453.3 mL/kg*min.

The PK of ShK-186 (Fig. 1C) and ShK-198 (Fig. 1D) following a single subcutaneous administration to monkey demonstrated a linear relationship between dose and both AUC and C_{max} (slope=1.02 – 1.27, R^2=0.97, Fig. 1F) through the entire range of doses from 35 to 1000 µg/kg. The monkey half-life ranged from 8.8 – 23.8 min for ShK-186 and from 16.7 – 73.5 min for ShK-198. Clearance rates in the monkey were generally lower for ShK-198 than ShK-186 and ranged from 18.7 to 141.3 mL/kg*min (Table 1 and 2).

These data indicate that ShK-186 and its metabolite ShK-198 reach a maximum concentration in plasma 1 to 15 min following a single subcutaneous injection of drug in both species, and both are rapidly cleared from the central compartment. The LOQ of the HPLC-MS method is approximately 10-fold higher than the IC_{50} of ShK-186 and ShK-198 on the Kv1.3 channel and thus lacks the sensitivity to estimate the terminal elimination phase at low but potentially therapeutic concentrations.

Absorption, distribution, metabolism, excretion (ADME) studies with a radiolabeled analog of ShK-186. We developed a radiolabeled analog of ShK-186 to measure the biodistribution of the peptide and evaluate its total concentration in whole blood. ShK-186 contains a single iodinatable tyrosine at position 23. However, iodine incorporation into the ring, which is predicted to interact within the pore region of the Kv1.3 channel (Pennington et al.,

1996), results in disruption of the channel binding properties of the peptide. We therefore modified the amino terminus of ShK-198 with a six-carbon linker attached via a peptide bond to one of the carboxylic acids of a DOTA chelate (Suppl. Fig. 2A). The DOTA-conjugate, designated ShK-221, was readily coordinated with indium or gadolinium (Suppl. Fig. 2B-C). In patch-clamp experiments, the gadolinium- and indium-labeled ShK-221 peptides blocked Kv1.3 with IC_{50} values similar to ShK-186 and ShK-198: Gd-ShK-221 (58.23 ± 1.38 pM; n=5), In-ShK-221 (63.8 ± 2.25 pM; n=3), ShK-186 (68.99 ± 4.01 pM; n=5) and ShK-198 (41.4 ± 7.25 pM; n=5) (Fig. 2C). We prepared and administered ^{111}In-labeled ShK-221 by subcutaneous injection to Sprague Dawley rats (1.0 mCi, 100 µg/kg) and squirrel monkeys (0.83 mCi, 35 µg/kg). The radiolabeling efficiency ranged from 89-98% over the series of experiments as determined by HPLC. Biodistribution of radiolabeled ShK-221 was evaluated by SPECT imaging continuously for the first hour post-dose, and then at 4, 8, 24, 48, 72, 120, and 160 h (Suppl. Videos 1-12). The background level in the detection system was approximately 0.1µCi/mL (~5 ng/mL of ShK-221 at the initial time point and 26 ng/mL at the last time point). Blood samples were collected following each scan, and total radioactivity in whole blood was measured by gamma counting. Computed tomography was performed at each time point to enable colocalization of the radiolabel with key anatomical structures.

Studies in squirrel monkeys. Biodistribution of ^{111}In-ShK-221 in squirrel monkeys was characterized principally by slow absorption from the injection site over the entire 160 h period (Fig. 3A and E). The quantity of ^{111}In-ShK-221 present at the injection site followed a biphasic exponential decay (R^2=0.95) with an initial half-life of approximately 1-1.5 h and a terminal half-life of >48 h (Fig. 3E). During the first hour, significant radioactivity could be observed in the kidney, increasing in intensity through 1 h [~1% injected dose (ID)/g, Suppl. Table 1] and slowly declining to approximately baseline by 48 h. Radioactivity in the monkey kidney was primarily observed in the cortical and medullary regions during all time points and was comparatively

16

absent in the renal pelvis except for the first hour (Fig. 3B). Significant bladder associated

radioactivity (T_{max}=0.75 − 1 h, 0.34 %ID/g) was only observed during the first 4 h, after which

relatively little radiolabel was detected in bladder. No other organ showed significant levels of

radioactivity except for liver, which peaked at 0.75 - 1 h post dose administration (0.166 %ID/g).

Muscle, heart and brain all had <0.1 %ID/g at all the time points measured (Suppl. Table 1).

Evaluation of blood-associated radioactivity in monkey at each time point also demonstrated a

biphasic exponential decay (R^2=0.99) with an initial half-life of approximately 1 h and a terminal

half-life of >64 h (Fig. 3F). In monkey much of the terminal elimination phase was reflected by

blood concentrations of ^{111}In-ShK-221 (>200 pM) well above the IC_{50} for ShK-186 (69 pM) and

ShK-198 (41 pM) and In-ShK-221 (64 pM) for 6 days post-dose. Even though ultrafiltration

studies demonstrate significant binding of ShK-186 to plasma proteins, the channel-blocking

activity of ShK-186 and In-ShK-221 are unaffected by the presence of serum (Fig. 2B and 2D-

E), suggesting that the bulk of the peptide detected in blood is functionally active.

Studies in rats. Biodistribution of ^{111}In-ShK-221 in the rat was similar to monkey and

characterized by slightly faster absorption from the injection site and excretion through the urine

over the first 24 h (Fig. 3C and E). Significant radioactive label was observed in rat bladder (9.4

%ID/g), kidney (2.9 %ID/g) and liver (0.4 %ID/g) during the first hour (Fig. 3C, Suppl. Table 2).

While little label was identified in the bladder at later time points, the amount of drug in liver and

kidney was relatively constant through the first 24 h. Cross-sectional views of the rat kidney

showed that, with the exception of the first hour, radioactivity was concentrated primarily in the

cortical regions similar to the monkey (Fig. 3D).

The whole blood-associated radioactivity in the rat also showed a biphasic exponential decay

(R^2=0.99) with an initial half-life of approximately 1.7 h and a terminal half-life of >72 h (Fig. 3F).

The ShK-221 concentrations in the rat (200 pM) were well above the IC_{50} for ShK-186 and ShK-

198 until 5 days post dose. In summary, the biodistribution of radiolabeled ShK-221 in squirrel

monkey and rat is characterized by a slow absorption from the injection site, significant concentrations of drug peripherally in the injection site, kidney, and liver and a long terminal elimination phase in whole blood.

Suppression of cytokine responses in human PBMCs. Another way that ShK-186 could exert a durable PD effect is through a sustained interaction with the Kv1.3 channel on lymphocytes. We therefore assessed the duration of lymphocyte suppression following exposure to ShK-186. We have previously shown that ShK-186 suppresses thapsigargin-induced expression of IL-2, IL-17, IFNγ, and IL-4 in freshly isolated human PBMCs (Chi et al., 2011). Here, we exposed PBMCs to the drug either continuously during a 48 h period of thapsigargin stimulation, for 1 h prior to 48 h of stimulation, or for 1 h up to 16 h prior to stimulation, and measured the IL-2 responses by ELISA (Fig. 4). In cases of transient exposure, the cells were thoroughly washed with media prior to thapsigargin treatment. There was no statistically significant difference (one-way ANOVA, $F(3,12)=0.40$, $p=0.76$) between continuous drug treatment versus transient drug exposure up to 16 h prior to thapsigargin stimulation. These data are consistent with a model where ShK-186 rapidly associates with but slowly dissociates from the Kv1.3 channel of lymphocytes.

Suppression of the DTH response *in vivo*; dose frequency and dose-response studies. Our ADME studies suggested that a low but therapeutically relevant drug concentration persists in the blood for several days following a single administration of ShK-186. We therefore evaluated the relationship between dose frequency and therapeutic efficacy in animal models of effector-memory T cell-mediated disease. The simplest model for assessing drug effects is the DTH reaction, an immune response largely mediated by skin-homing effector-memory CD4^{+} T cells (Soler et al., 2003; Matheu et al., 2008). We immunized groups of 5 – 8 Lewis rats with OVA in complete Freund's adjuvant (CFA) followed 7 – 9 days later by elicitation of the DTH response in the ears of immunized animals. Ear swelling was measured 24 h post-elicitation.

The durability of drug effect was assessed by treating animals with ShK-186 at varying times prior to or coincident with the elicitation phase. The day of ear challenge is referred to as Day 0 for reference.

Animals that were treated with two doses of 10 or 100 µg/kg ShK-186 on Day 0 and Day 1 (the standard regimen) were compared with single 100 µg/kg doses administered on Days 0, -1, -2, -3, or -4. Two doses administered on Day 0 and 1 and single doses administered on Days -1 through -4 yielded statistically significant reductions in ear swelling relative to placebo-treated animals (two-tailed Mann-Whitney test, Fig. 5A). Single doses administered prior to Day -4 did not result in a significant reduction in ear swelling relative to the control group (data not shown). We conclude that a single subcutaneous injection of ShK-186 is sufficient to suppress the DTH response in rat for a period of 5 days, consistent with the long terminal elimination half-life of radiolabeled ShK-221.

In order to establish a relationship between dose-level and the time of dosing, we evaluated the suppressive effect of a single ascending dose (0.1 - 100 µg/kg) of ShK-186 administered 2 days prior to ear challenge. A dose-dependent reduction in ear swelling was observed over the 3-log dose range, with doses ≥1 µg/kg achieving statistical significance relative to vehicle-treated animals (Fig. 5B).

Treatment strategies in the CR-EAE and PIA models. CR-EAE is widely used as a model of multiple sclerosis. This model was extensively characterized in guinea pigs (Raine et al., 1977; Keith et al., 1979) and more recently in DA rats (Feurer et al., 1985; Lorentzen et al., 1995) and unlike the acute EAE models includes relapses and some degree of demyelination (Lassman and Wisniewsky, 1979; Lorentzen et al., 1995; Matheu et al., 2008). Moreover, due to its protracted nature, it is an adequate model for testing dosing schedules. The initial wave of disease is largely adjuvant mediated and composed primarily of central memory T cells, whereas subsequent waves of disease are principally T_{EM} cell-mediated and therefore Kv1.3-

dependent (Matheu et al., 2008). We have previously shown ShK-186 to be effective in the CR-EAE model using daily dosing at 100 µg/kg (Matheu et al., 2008). In the present study, we explored the effect of less frequent dose administration on drug efficacy in this model.

Two study designs were explored. In the first, a lead-in period with daily drug administration was initiated at the time of disease induction and continued throughout the first wave of disease. Seven days following disease onset, animals were randomized to receive 100 µg/kg ShK-186 every 2 or 3 days through the remainder of the study. Daily drug treatment caused a statistically significant reduction in mean clinical score compared to placebo treated animals during the first wave of disease (Fig. 6A). Following lead-in, drug administration every 2 or 3 days resulted in continued significantly lower mean daily clinical score in treated relative to control animals. The average cumulative clinical score was 161.1±162.3, 72.5±98.1, and 71.3±103.3 for the placebo, every-2-day, and every-3-day dosing groups, respectively. Animals were scored twice daily.

In a second series of experiments, we evaluated the effect of reduced dose frequency on EAE without the drug lead-in period. In this study, groups of DA rats were randomized to receive placebo, daily ShK-186, or ShK-186 every three days beginning at a clinical score ≥1. Both drug-treated groups exhibited a significantly lower mean daily clinical score than placebo-treated animals (Fig. 6B). However, there was no statistically significant difference between daily and every-third-day dose administration. Mean cumulative clinical scores were 49.7±26.7, 36.9±20.6, and 30±19.3 for the placebo, daily, and every third day dosing groups respectively. The percentage of rats with one or more relapses was 70% (9/13), 21% (3/14) and 21% (3/14), and the total number of relapses observed during the chronic phase were 15, 6 and 5 for the placebo treated, ShK186 daily, and every three day treated groups, respectively. Animals were scored once daily.

Finally, we wished to evaluate the durability of disease suppression in the CR-EAE model following cessation of drug administration. Disease was elicited in groups of DA rats and the

20

animals were allowed to develop a relapsing disease. On day 10 following disease onset (clinical score ≥1), animals were randomized to receive daily placebo or 100 µg/kg ShK-186 for a period of 14 days. Drug treatment was discontinued on Day 24, and the animals were monitored for an additional 15 days. There was no difference between the placebo and drug-treated groups prior to drug treatment (Fig. 6C). During the 14 days of daily drug administration, there was a statistically significant reduction in mean clinical score in drug treated versus control animals. Once treatment was withdrawn, the mean clinical score in the drug treated group slowly returned to the level of placebo over a period of approximately 5 days (Suppl. Table 3). However, there was no rebound effect observed in the previously-treated animals.

As a final test of the effectiveness of less than daily dosing, we evaluated ShK-186 administration every other day in the PIA model of rheumatoid arthritis (Beeton et al., 2006). ShK-186 administered once daily (100 µg/kg) has been previously reported to reduce the number of joints affected and the severity of joint swelling in the PIA model in DA rats (Beeton et al., 2006). Here, we demonstrate that ShK-186 administered on alternate days (100 µg/kg) was as effective in ameliorating disease (Fig. 7) as our previously reported effect with once daily administration (Beeton et al., 2006).

The data from these four studies are consistent with a model of durable drug effects following a single subcutaneous dose of ShK-186 and are consistent with observations made using the DTH model.

DISCUSSION

Here, we present five complementary types of data that relate the PK properties of ShK-186 to its therapeutic efficacy in rat models of autoimmune diseases. Through serum/plasma stability studies, we identify the sole metabolite of ShK-186 in rat, monkey and human samples as the dephosphorylated peptide, ShK-198. ShK-198 blocks Kv1.3 (IC_{50} 40 pM) with roughly the same potency as ShK-186 (69 pM). Second, we demonstrate that the C_{max} of both ShK-186 and ShK-198 are rapidly reached following subcutaneous injection to rat and monkey. Both parent and metabolite have a short apparent half-life in the central compartment with >90% of the C_{max} eliminated by 2 h in both species at all tested doses. The half-life is shorter and the apparent clearance greater for ShK-186 than ShK-198, likely reflecting the independent action of endogenous phosphatases on the conversion of ShK-186 to its metabolite. Third, SPECT imaging of rats and monkeys administered an ^{111}In-labeled ShK-186 analog (ShK-221, IC_{50} 65 pM) by subcutaneous injection revealed that the peptide is released slowly from the injection site, and has an extended terminal half-life, with whole-blood levels above the IC_{50} value for Kv1.3 block for 5 days in rats and 7 days in monkeys. The Kv1.3 channel-blocking affinity of ShK-186 and ShK-221 is not affected by the presence of serum indicating that plasma protein binding, if any, does not affect the functional activity of these peptides. Fourth, *in vitro* proliferation assays demonstrate that brief 1 h exposure of PBMCs to ShK-186 is sufficient to suppress interleukin 2 production 64 h later. This suggests that the peptide, once bound to the Kv1.3 channel, dissociates very slowly. Finally, in three different rat models of T_{EM} cell-mediated inflammatory diseases—DTH, CR-EAE, and PIA—ShK-186 is as effective in ameliorating disease when administered every 2-5 days as when it is administered once daily. The durable PD effect of ShK-186 is contrary to conventional wisdom that frequent administration of peptide therapeutics is required to sustain PD activity.

Our findings highlight a potential advantage of developing peptides from venoms as drug candidates. SPECT imaging studies with ^{111}In-labeled ShK-221 revealed a biphasic (fast then slow) release from the subcutaneous injection site over 7 days in rats and monkeys. This type of rate-limiting absorption resulting in prolonged plasma exposure has been described for whole animal venoms (Audebert et al., 1994; Barral-Netto et al., 1990). The long absorption phase has been used to explain the frequent relapse in envenomation patients long after exposure and/or treatment with antivenom (Dart et al., 2001; Guittierrez et al., 2003, Seifert and Boyer, 2001), and venoms are often described as having a depot effect. The parent peptide of ShK-186 was originally isolated from the venom of *Stichodactyla helianthus* (Castenada et al., 1995), and ShK-186 may share some of the *in vivo* characteristics of the complex peptide mixtures found in animal venom. Venom and toxin PK parameters are also characterized by large apparent volumes of distribution and slow elimination from deep and shallow peripheral compartments (Ismail et al., 1996).The apparent volume of distribution for ShK-186 is large in both rat (2743 – 16458 mL/kg) and monkey (1729 – 2664 mL/kg), consistent with that reported for other animal venoms. The blood concentration of ^{111}In-ShK-221 mimicked the absorption of the peptide from the injection site and was characterized by a rapid initial phase and a very long terminal phase. The terminal half-life computed using ^{111}In-ShK-221 was >64 h in monkey with sustained blood levels for 7 days above the IC_{50} values for ShK-186 (69 pM) and ShK-198 (40 pM). The presence of serum does not affect channel-blocking affinity of these peptides, indicating that plasma protein binding, if any, does not affect functional activity.

Glomerular filtration is the principal elimination pathway for the peptide shortly after subcutaneous injection. Significant amounts of radioactivity were observed in the bladder of both rat (~17 % injected dose) and monkey (~1% injected dose) at the earliest time points following administration of ^{111}In-ShK-221. The large amount of drug excreted by the rat in the first hour is most likely a reflection of the increased metabolism of the rat compared to the

monkey. Following 1 h in rat and approximately 4 h in monkey, little radioactivity is observed in bladder or renal pelvis whereas significant amounts of radioactivity can still be observed in the kidney cortex. Cortical concentration has been reported for numerous radiolabeled versions of peptide drugs including octreotide, bombesin, exendin, and gastrin (Gotthardt et al., 2007). The mechanism of cortical retention has been most thoroughly described for octreotide. Tubular reabsorption of the cationic octapeptide is mediated by megalin, a scavenger receptor expressed in the proximal kidney tubule (de Jong et al., 2005). Mice with a kidney-specific disruption of the receptor lack the cortical retention of radiolabeled octreotide seen in wild-type mice. Renal uptake of octreotide is partially mediated by charge and can be disrupted by co-infusion of the positively charged amino acids L-lysine and L-arginine (Bodei et al., 2003). ShK-186 carries a net +6 charge at physiological pH, and so its cortical retention may be mediated by a similar mechanism.

Another contributing factor to the long PD effect of ShK-186 along with an extended terminal half-life could be its slow dissociation from the Kv1.3 channel. Studies with PBMCs show that there is essentially no difference between continuous ShK-186 treatment during thapsigargin-stimulation and treatment up to 16 h prior to stimulation. While we did not formally measure an off-rate of the drug on the Kv1.3 channel using traditional methods, we did show that ShK-186's PD effect can persist for at least 72 hours after its brief exposure to PBMCs. The receptor dissociation half-life of some animal toxins has been reported to be as long as one week (Berg and Hall 1975, Chang and Huang 1975). Future receptor binding studies using the radiolabeled analog will allow determination of the off-rate of ShK-186 from Kv1.3.

ADME studies with ^{111}In-labeled ShK-221 suggest that a single dose of peptide can provide therapeutically meaningful blood concentrations for up to 5 days in rat and 7 days in monkey. These data are consistent with data from the rat DTH model where a single administered dose of ShK-186 provided a statistically significant reduction in ear swelling for up to five days.

Likewise, dose administration every 2-3 days in the CR-EAE and PIA models were as effective in ameliorating disease as daily ShK-186 administration. Since ShK-186's therapeutic effects are long lasting, we anticipate administering the peptide to humans once weekly or less frequently. From a therapeutic and commercial perspective, ShK-186 will compete favorably with daily or multiple times/day pills or injectables.

AUTHORSHIP CONTRIBUTIONS

Participated in research design: Bailey, Beeton, Boley, Chandy, Chi, Iadonato, Knapp, Muñoz-Elías, Pennington, Slauter, Tarcha, Rupert

Conducted experiments: Bailey, Beeton, Chi, Hansen, Hu, Iadonato, Kentala, Muñoz-Elías, Nguyen, Norton, Banks, Tarcha, Tjong, Upadhyay

Contributed new reagents or analytical tools: Bailey, Pennington, Tarcha

Performed data analysis: Bailey, Beeton, Chandy, Chi, Iadonato, Knapp, Muñoz-Elías, Nguyen, Tarcha, Upadhyay

Wrote or contributed to the writing of the manuscript: Iadonato; Tarcha, Muñoz-Elías, Chi, Chandy (sections contributed)

REFERENCES

Audebert F, Urtizberea M, Sabouraud A, Scherrmann J-M, and Bon C (1994) Pharmacokinetics of *Vipera aspis* venom after experimental envenomation in rabbits. *J Pharmacol Exp Ther* **268:**1512-1517.

Azam P, Sankaranarayanan A, Homerick D, Griffey S, and Wulff H (2007) Targeting effector memory T cells with the small molecule Kv1.3 blocker PAP-1 suppresses allergic contact dermatitis. *J Invest Dermatol* **127:**1419-1429.

Barral-Netto M, Schriefer A, Vinhas V, and Almeida AR (1990) Enzyme-linked immunosorbent assay for the detection of *Bothrops jararaca* venom. *Toxicon* **28:** 1053-1061.

Beeton C, Wulff H, Barbaria J, Clot-Faybesse O, Pennington M, Bernard D, Cahalan MD, Chandy KG, and Beraud E (2001) Selective blockade of T lymphocyte K$^+$ channels ameliorates experimental autoimmune encephalomyelitis, a model for multiple sclerosis. *PNAS* **98:**13942-13947.

Beeton C, Pennington MW, Wulff H, Singh S, Nugent D, Crossley G, Khaytin I, Calabresi PA, Chen C-Y, Gutman GA, and Chandy KG (2005) Targeting effector memory T cells with a selective peptide inhibitor of Kv1.3 channels for therapy of autoimmune diseases. *Mol Pharmacol* **67:**1369-1381.

Beeton C, Wulff H, Standifer NE, Azam P, Mullen KM, Pennington MW, Kolski-Andreaco A, Wei E, Grino A, Counts DR, Wang PH, LeeHealey CJ, Andrew BS, Sankaranarayanan A, Homerick D, Roeck WW, Tehranzadeh J, Stanhope KL, Zimm P, Havel PJ, Griffey S, Knaus H-G, Nepom GT, Gutman GA, Calabresi PA, and Chandy KG (2006) Kv1.3 channels are a therapeutic target for T cell-mediated autoimmune diseases. *PNAS* **103**: 17414-17419.

Beeton C, and Chandy KG (2007). Induction and monitoring of active delayed type hypersensitivity (DTH) in rats. *J Vis Exp* **6:**http://www.jove.com/Details.htm?ID=237&VID=233.

26

Berg DK and Hall ZW (1975) Loss of α-bungarotoxin from junctional and extrajunctional acetylcholine receptors in rat diaphragm muscle *in vivo* and in organ culture. *J Physiol Lond* **252:**771-789.

Bodei L, Cremonesi C, Zoboli S, Grana C, Bartolomei M, Rocca P, Caracciolo M, Macke HR, Chinol M, and Paganelli G (2003) Receptor-mediated radionuclide therapy with 90Y-DOTATOC in association with amino acid infusion: a phase 1 study. *Eur J Nucl Med Mol Imaging* **30:**207-216.

Cahalan MD, and Chandy KG. The functional network of ion channels in T lymphocytes. (2009) *Immunol Rev* **231:**59-87.

Castenada O, Sotolongo V, Amor AM, Stocklin R, Anderson AJ, Harvey AL, Engstrom A, Wernstedt C, and Karlsson E (1995) Characterization of a potassium channel toxin from the Caribbean sea anemone *Stichodactyla helianthus. Toxicon* **33:**603-613.

Chang CC and Huang MC (1975) Turnover of junctional and extrajunctional acetylcholine receptors of rat diaphragm. *Nature* **253:** 643-644.

Chi V, Pennington MW, Norton RS, Tarcha EJ, Londono LM, Sims-Fahey B, Upadhyay SK, Lakey JT, Iadonato S, Wulff H, Beeton C, and Chandy KG (2011) Development of a sea anemone toxin as an immunomodulator for therapy of autoimmune diseases. *Toxicon* In press.

Choeng A, Li J, Sukumar P, Kumar B, Zeng F, Riches K, Munsch C, Wood IC, Porter KE, and Beech DJ (2011) Potent suppression of vascular smooth muscle cell migration and human neointimal hyperplasia by Kv1.3 blockers. *Cardiovasc Res* **89:**282-289.

Dart RC, Seifert SA, Boyer LV, Clark RF, Hall E, McKinney P, McNally J, Kitchens CS, Curry SC, Bogdan GM, Ward SB, and Porter RS (2001). A randomized multicenter trial of Crotalinae polyvalent immune Fab (ovine) antivenom for the treatment for crotaline snakebite in the United States. *Arch Intern Med* **161**: 2030–2036.

De Jong M, Barone R, Krenning E, Bernard B, Melis M, Visser T, Gekle M, Willnow T, Walrand S, Jamar F, and Pauwels S (2005) Megalin is essential for renal proximal tubule reabsorption of ^{111}In-DTPA-Octreotide. *J Nucl Med* **46:**1696-1700.

Feurer C, Prentice DE, and Cammisuli S (1985) Chronic relapsing experimental allergic encephalomyelitis in the Lewis rat. *J Neuroimmunol* **10:**159-166.

Gilhar A, Bergman R, Assay B, Ullmann Y, and Etzioni A (2011) The beneficial effect of blocking Kv1.3 in the psoriasiform SCID mouse model. *J Invest Dermatol* **131:**118-124.

Gillett A, Marta M, Jin T, Tuncel J, Leclerc P, Nohra R, Lange S, Holmdahl R, Olsson T, Harris RA, and Jagodic M (2010) TNF production in macrophages is genetically determined and regulates inflammatory disease in rats. *J Immunol* **185:**442-450.

Gotthardt M, van Eerd-Vismale J, Wim JG, de Jong M, Zhang H, Rolleman E, Maecke HR, Behe M, and Boerman O (2007) Indication for different mechanisms of kidney uptake of radiolabeled peptides. *J Nucl Med* **48:**596-601.

Grgic I, Wulff H, Eichler C, Flothmann R, Kohler R, and Hoyer J (2009) Blockade of T-lymphocyte KCa3.1 and Kv1.3 channels as novel immunosuppression strategy to prevent kidney allograft rejection. *Transplantation Proceedings* **41:**2601-2606.

Gutierrez JM, Leon G, and Lomonte B (2003) Pharmacokinetic–pharmacodynamic relationships of immunoglobulin therapy for envenoming. *Clin Pharmacokinet* **42**: 721–741.

Hill AV (1910) The possible effects of the aggregation of the molecules of haemoglobin on its dissociation curves. *J. Physiol* **40**: i-vii.

Hu L, Pennington M, Jiang Q, Whartenby KA, and Calabresi PA (2007) Characterization of the functional properties of the voltage-gated potassium channel Kv1.3 in human CD4+ T lymphocytes. *J Immunol* **179**:4563-4570.

Hu L, Gocke AR, Knapp E, Rosenzweig JM, Grishkan IV, Baxi EG, Zhang H, Margolick JB, Whartenby KA, and Calabresi PA (2012) Functional blockade of the voltage-gated

potassium channel Kv1.3 mediates reversion of T effector to central memory lymphocytes through SMAD3/p21cip1 signaling. *J Biol Chem* **287**:1261-1268.

Hyodo T, Oda T, Kikuchi Y, Higashi K, Kushiyama T, Yamamoto K, Yamada M, Suzuki S, Hokari R, Kinoshita M, Seki S, Fujinaka H, Yamamoto T, Miura S, and Kumagai H (2010) Voltage gated potassium channel Kv1.3 blocker as a potential treatment for rat anti-glomerular basement membrane glomerulonephritis. *Am J Physiol Renal Physiol* **299:**F1258-1269.

Ismail M, Aly HMH, Abd-Elsalam MA, and Morad AM (1996) A three-compartment open pharmacokinetic model can explain variable toxicities of cobra venom and their alpha toxins. *Toxicon* **34:**1011-1026.

Keith AB, Arnon R, Teitelbaum D, Caspary EA, and Wisniewski HM (1979) The effect of Cop 1, a synthetic polypeptide, on chronic relapsing experimental allergic encephalomyelitis in guinea pigs. *J Neurol Sci* **42**:267-274.

Koo GC, Blake JT, Talento A, Nguyen M, Lin S, Sirotina A, Shah K, Mulvany K, Hora D, Cunningham P, Wunderler DL, McManus OB, Slaughter R, Bugianesi R, Felix J, Garcia M, Williamson J, Kaczorowski G, Sigal NH, Springer MS, and Feeney W (1997) Blackade of the voltgage gated potassium channel Kv1.3 inhibits immune responses *in vivo. J Immunol* **158:**5120-5128.

Lassmann H, Wisniewski HM (1979) Chronic relapsing experimental allergic encephalomyelitis: effect of age at the time of sensitization on clinical course and pathology. *Acta Neuropathol* **47:**111-116.

Lorentzen JC, Issazadeh S, Storch M, Mustafa MI, Lassman H, Linington C, Klareskog L, and Olsson T (1995) Protracted, relapsing and demyelinating experimental autoimmune encephalomyelitis in DA rats immunized with syngeneic spinal cord and incomplete Freund's adjuvant. *J Neuroimmunol* **63:**193-205.

Matheu MP, Beeton C, Garcia A, Chi V, Rangaraju S, Safrina O, Monaghan K, Uemura MI, Li D, Pal S, de la Maza LM, Monuki E, Flugel A, Pennington MW, Parker I, Chandy KG, and Cahalan MD (2008) Imaging of effector memory T cells during a delayed-type hypersensitivity reaction and suppression by Kv1.3 channel blockade. *Immunity* **29:**602-614.

McCloskey C, Jones S, Amisten S, Snowden RT, Kaczmarek LK, Erlinge D, Goodall AH, Forsythe ID, and Mahaut-Smith MP (2010) Kv1.3 is the exclusive voltage-gated K+ channel of platelets and megakaryocytes: roles in membrane potential, Ca2+ signaling and platelet count. *J Physiol* **588:**1399-406.

Pennington MW, Mahnir VM, Zaydenberg I, Byrnes ME, and Kem WR (1996) An essential binding surface for ShK toxin interaction with rat brain potassium channels. *Biochemistry* **35:**16407-16411.

Pennington MW, Beeton C, Galea CA, Smith BJ, Chi V, Monaghan KP, Garcia A, Rangaraju S, Giuffrida A, Plank D, Crossley G, Nugent D, Khaytin I, Lefievre Y, Peshenko I, Dixon C, Chauhan S, Orzel A, Inoue T, Hu X, Moore RV, Norton RS, Chandy KG. (2009). Engineering a stable and selective peptide blocker of the Kv1.3 channel in T lymphocytes. *Mol Pharmacol.* **75**:762-73.

Raine CS, Snyder DH, Stone SH, and Bornstein MB. (1977) Suppression of acute and chronic experimental allergic encephalomyelitis in Strain 13 guinea pigs. A clinical and pathological study. *J Neurol Sci* **33**:355-367.

Rangaraju S, Chi V, Pennington MW, and Chandy KG (2009) Kv1.3 potassium channels as a therapeutic target in multiple sclerosis. *Expert Opin Ther Targets* **13:**1-17.

Rintisch C, Förster M, Holmdahl R. (2009). Detection of arthritis-susceptibility loci, including Ncf1, and variable effects of the major histocompatibility complex region depending on genetic background in rats. *Arthritis Rheum* **60:**419-427.

Rus H, Pardo, CA, Hu L, Darrah E, Cudrici C, Niculescu T, Niculescu F, Mullen KM, Allie R, Guo L, Wulff H, Beeton C, Judge SIV, Kerr DA, Knaus H-G, Chandy KG, and Calabresi PA

(2005) The voltgage-gated potassium channel Kv1.3 is highly expressed on inflammatory brain infiltrates in multiple sclerosis brain. *PNAS* **102:**11094-11099.

Seifert SA and Boyer LV (2001) Recurrence phenomena after immunoglobulin therapy for snake envenomations: part 1. Pharmacokinetics and pharmacodynamics of immunoglobulin antivenoms and related antibodies. *Ann Emerg Med* **37:** 189-195.

Soler D, Humphreys TL, Spinola SM, and Campbell JJ (2003) CCR4 versus CCR10 in human cutaneous Th lymphocyte trafficking. *Blood* **101:**1677-1682.

Trowbridge EA, Martin JF, Slater DN, Kishk YT, Warren CW, Harley PJ, Woodcock B (1984) The origin of platelet count and volume. *Clin Phys Physiol Meas* **5:**145-70.

Wulff H, Calabresi PA, Allie R, Yun S, Pennington M, Beeton C, and Chandy KG (2003) The voltage-gated Kv1.3 K+ channel in effector memory T cells as new target for MS. *J Clin Invest* **111:**1703-1713.

Wulff H, Miller MJ, Hansel W, Grissmer S, Cahalan MD, Chandy KG (2000) Design of a potent and selective inhibitor of the intermediate-conductance Ca^{2+}-activated K^+ channel, IKCa1: A potential immunosuppressant. *PNAS* **97**:8151-8156.

FOOTNOTES

FIGURE LEGENDS

FIGURE 1. Pharmacokinetic profiles of ShK-186 and ShK-198 in plasma following a single dose to rat and monkey. ShK-186 was administered by subcutaneous injection to Sprague Dawley rats (**A** and **B**, n=3-9 animals/dose/time point) and cynomolgus monkeys (**C** and **D**, n=2-16 animals/dose/time point) and plasma samples were collected at time intervals ranging from 1 minute to 24 hours. Samples were analyzed using a validated HPLC-MS/MS method that can resolve both the parent compound (ShK-186, **A** and **C**) and its metabolite (ShK-198, **B** and **D**). The C_{max} and $AUC_{0\text{-inf}}$ were computed for rat (**E**) and monkey (**F**) at each dose level using non-compartmental analysis and the linear trapezoidal method.

FIGURE 2. Biophysical Properties of ShK-186, ShK-186 dephosphorylated form (ShK-198), and ShK-186 analogs. (**A**) Representative whole cell Kv1.3 currents in the absence and presence of dephosphorylated ShK-186 (ShK-198). (**B**) Representative whole cell Kv1.3 currents in the absence and presence of In-ShK-221 (a ShK-186 analog). In-ShK-221 was in 100% serum. (**C**) Comparison of dose response curves for ShK-186, ShK-198, Gd-ShK-221, and In-ShK-221 on Kv1.3. The IC50 values were: ShK-186 = 68.99 ± 4.01 pM (n=5), ShK-198 = 41.4 ± 7.25 pM (n=5), Gd-ShK-221 = 58.23 ± 1.38 pM (n=5), In-ShK-221 = 63.8 ± 2.25 pM (n=3). (**D**) Dose response curves of ShK-186 on Kv1.3 in the presence of varying concentrations of serum. (**E**) Dose response curve of In-ShK-221 in the presence or absence of serum. Electrophysical recordings were carried out in the whole-cell configuration of the patch-clamp technique as described (Beeton et al. 2005 and Wulff et al. 2000). The external solution was sodium Ringer and the pipette solution was KF (300 mOsm). Kv1.3 currents were elucidated by 200-ms depolarizing pulses from a holding potential of -80 to 40 mV. All analogs were each tested at several concentrations. The reduction in peak current at 40 mV for each concentration was used to generate a dose-response curve using Origin software (OriginLab Corp., Northhampton, MA).

FIGURE 3. Biodistribution studies with radiolabeled ShK in rat and squirrel monkey. ^{111}In-labelled ShK-221 was administered to Sprague Dawley rat (100µg/kg; 1.0mCi) and squirrel monkey (35µg/kg; 0.84mCi) as a single subcutaneous injection to the scapular region of each animal. SPECT and CT scans were collected continuously during the first hour (4 x 15 m intervals) and at 4, 8, 24, 48, 72, 120, and 160 h post-dose. Flattened 2D images of the 3D reconstructions are shown for the 4, 24, 72 and 160 h time points for monkey (**A**) and the 1, 8 and 24 h time points for rat (**C**). Both animals show slow absorption of drug from the injection site and significant early and sustained distribution to kidney and to a lesser extent liver. Kidney associated radioactivity in both species was principally identified in the cortex (**B** and **D**). Quantification of ^{111}In-ShK-221 at the injection site in monkey (top) and rat (bottom) revealed a biphasic decay with an initial half-life of approximately 0.5 -1.5 h and a terminal half-life of >48 h (**E**). Drug concentrations in monkey (top) and rat (bottom) whole blood followed a similar biphasic decay with an initial half-life of approximately 1.5 h and a terminal half-life of >64 h (**F**). Blood concentrations remained above the IC_{50} for Kv1.3 throughout the entire study period and above the 80% saturation concentration (233 pM) through the first 120 h consistent with a slow, continuous distribution from the injection site throughout the study period.

FIGURE 4. Durable effect of drug treatment on human PBMCs. Time of treatment studies were conducted in human PBMCs where the effect of drug treatment timing and duration on thapsigargin-stimulated IL-2 responses was measured. Continuous drug treatment during the 48 h stimulation period (**A**, black bar) was compared with drug pretreatment for 1 h followed by a brief washout and stimulation for 48 h (**B**, open bar) or drug pretreatment (1 h) followed by washout, media incubation (16 h) and thapsigargin stimulation (48 h) (**C**, hatched bar). Drug treatment for a 1 h period up to 16 h prior to stimulation was statistically indistinguishable from continuous drug treatment. None of the treatment times and durations were significantly different (one-way ANOVA, $F(3,12)=0.40$, $p=0.76$). POC = Percent of Control.

FIGURE 5. Time of administration and dose-dependent suppression of the DTH response.

Lewis rats were immunized with ovalbumin in CFA and challenged 7 – 9 days later by injection of ovalbumin to the ear pinna. The day of challenge is represented as Day 0. The DTH reaction was measured 24 h post-challenge (Day 1). ShK-186 administered at 10 or 100 µg/kg in two doses on Day 0 and Day 1 or as a single 100 µg/kg dose on Day -1, -2, -3, and -4 resulted in a significant reduction in ear swelling relative to placebo-treated animals when measured on Day 1 post-challenge (**A**; two-tailed Mann-Whitney; * $p<0.05$, ** $p<0.01$). These data indicate that a single ShK-186 dose can suppress the DTH response for a period of up to 5 days. Using the DTH model, a dose-response study was conducted with a single dose of ShK-186 administered on Day -2 (**B**). Doses between 0.1 and 100 µg/kg show a clear dose-response relationship, with all but 0.1 µg/kg achieving statistical significance relative to placebo.

FIGURE 6. Alternate dosing schedules are effective in chronic EAE model. An initial study evaluated lead-in dosing followed by less than daily drug administration (**A**). Male DA rats were immunized with spinal cord homogenate in CFA and administered ShK-186 (100 µg/kg/day, n=25) or vehicle (n=12) during the prodromal period and for 7 days following onset of EAE, after which drug treated animals were randomized to receive a maintenance dose of 100 µg/kg ShK-186 every 2 (n=12) or 3 (n=13) days. ShK-186 significantly reduced ($p<0.001$) the severity of the initial episode of disease. Maintenance therapy administered at 48 or 72 h intervals significantly ($p<0.001$, one-way repeated measures ANOVA) reduced the severity of CR-EAE. A second study measured the effect of infrequent drug administration beginning at disease onset (**B**). Female DA rats (n=13/group) were immunized with spinal cord homogenate in CFA to elicit a chronic, relapsing EAE. Following onset of symptoms (clinical score >1), animals were randomized to receive daily placebo, daily ShK-186 or ShK-186 every 2 or 3 days. Drug treatment resulted in significantly lower clinical scores and a lower frequency of disease incidence (**inset**) during the chronic phase in the daily and every-third-day treated groups

compared with placebo (repeated measures ANOVA, $F_{(2,60)}=39.4$, $p<0.0001$). Mean clinical scores were not lower relative to placebo in the group treated on alternate days in this study (data not shown). A final study measured the durability of response of a period of drug therapy (**C**). Female DA rats (n=23) were immunized and allowed to proceed to CR-EAE. 10 days following the onset of symptoms, animals were randomized to receive daily placebo (n=10) or ShK-186 100 μg/kg (n=13) for 14 days. Therapy was discontinued on day 24 and the time required for treated animals to return to baseline disease was evaluated. The previously-treated group had mean clinical scores significantly lower than placebo controls on days 24, 25, 26, and 28 (Suppl. Table 2) consistent with a 5 day window for disease recurrence.

FIGURE 7. Pristane-induced arthritis treated with alternate day administration of ShK-186. Arthritis was induced in DA rats by injection of 75 μL of pristane at the base of the tail. Disease was allowed to evolve to a clinical score of 1 when animals were randomized to receive placebo or 100 μg/kg ShK-186 every other day. Clinical score is computed as per Gillett et al 2010. Overall disease severity in the study was high. Animals receiving ShK-186 every other day had a statistically significant reduction in mean score (placebo, 20.4±5.9; drug, 14.6±4.1; paired t-test, $p< 0.0001$).

TABLES

Table 1: ShK-186 pharmacokinetic parameters in Sprague Dawley rat and cynomolgus monkey

Species	Dose	N	T_{max}	$t_{½}$	C_{max}	$AUC_{0\text{-inf\_obs}}$	Cl
Cyno	35	10	5	8.8	12.8	247.6	141.3
	100	14	5	14.5	33.6	823.1	121.8
	150	16	5	23.8	69.8	1935.9	78.5
	250	2	5	11.3	106.6	2220.9	112.2
	300	5	5	14.0	173.8	3496.4	86.0
	500	2	5	15.8	192.5	4734.0	105.6
	1000	2	5	13.0	358.0	9552.7	104.6
SD Rat	50	6	1	4.4	26.2	115.9	441.4
	150	6	1	9.2	27.0	249.5	640.9
	250	3	5	4.7	29.7	282.9	886.3
	500	9	1	5.2	42.7	587.5	847.2
	1000	3	5	7.9	48.0	690.6	1453.3

Table 2: ShK-198 pharmacokinetic parameters in Sprague Dawley rat and cynomolgus monkey

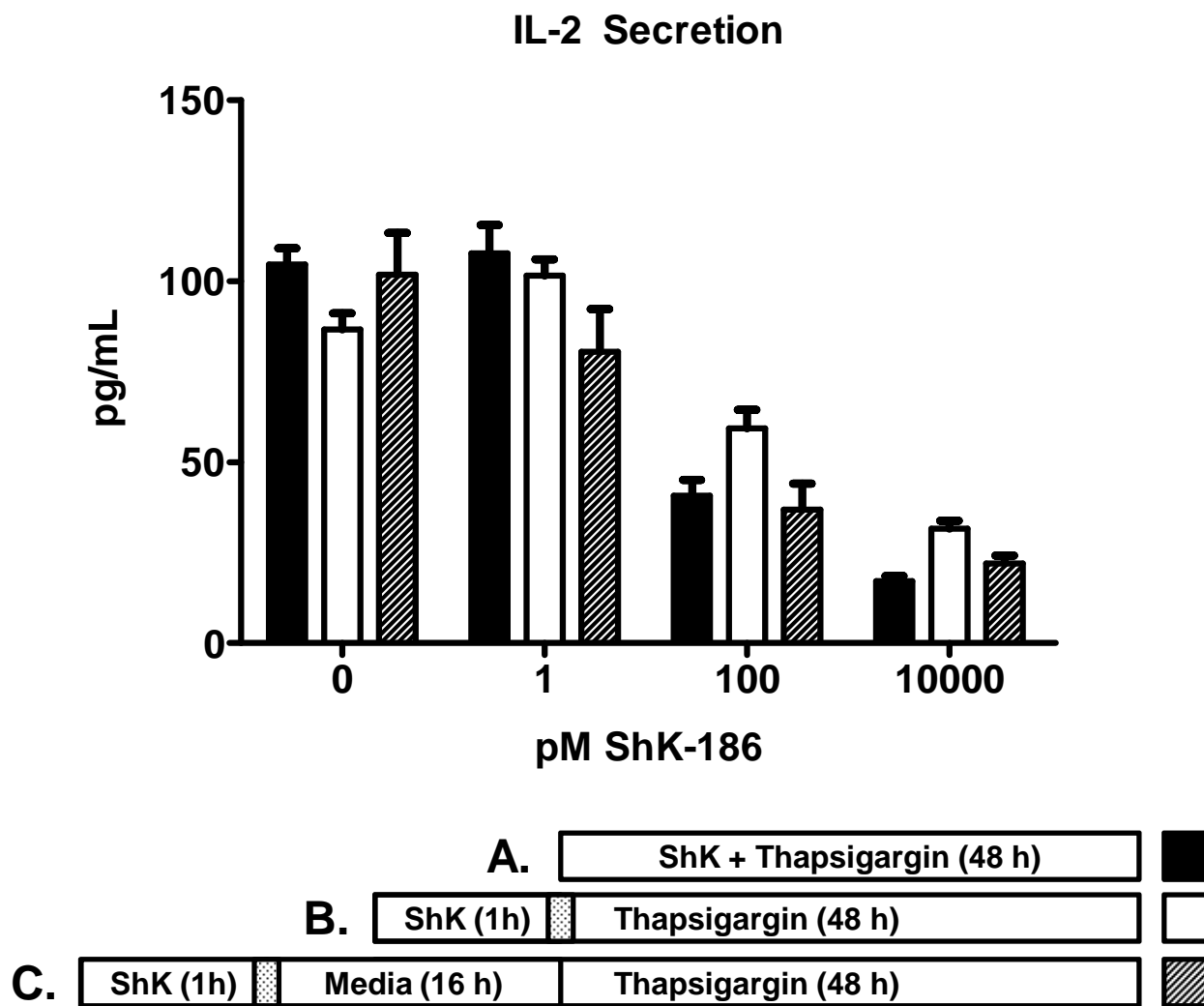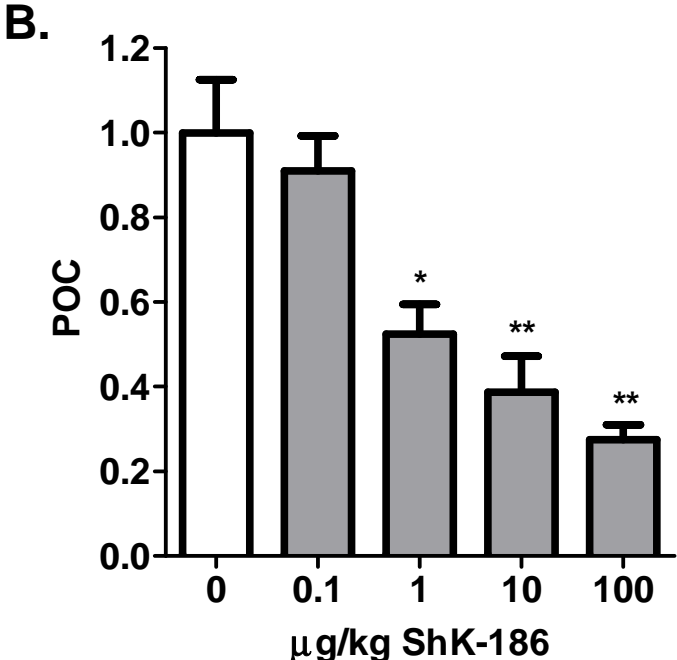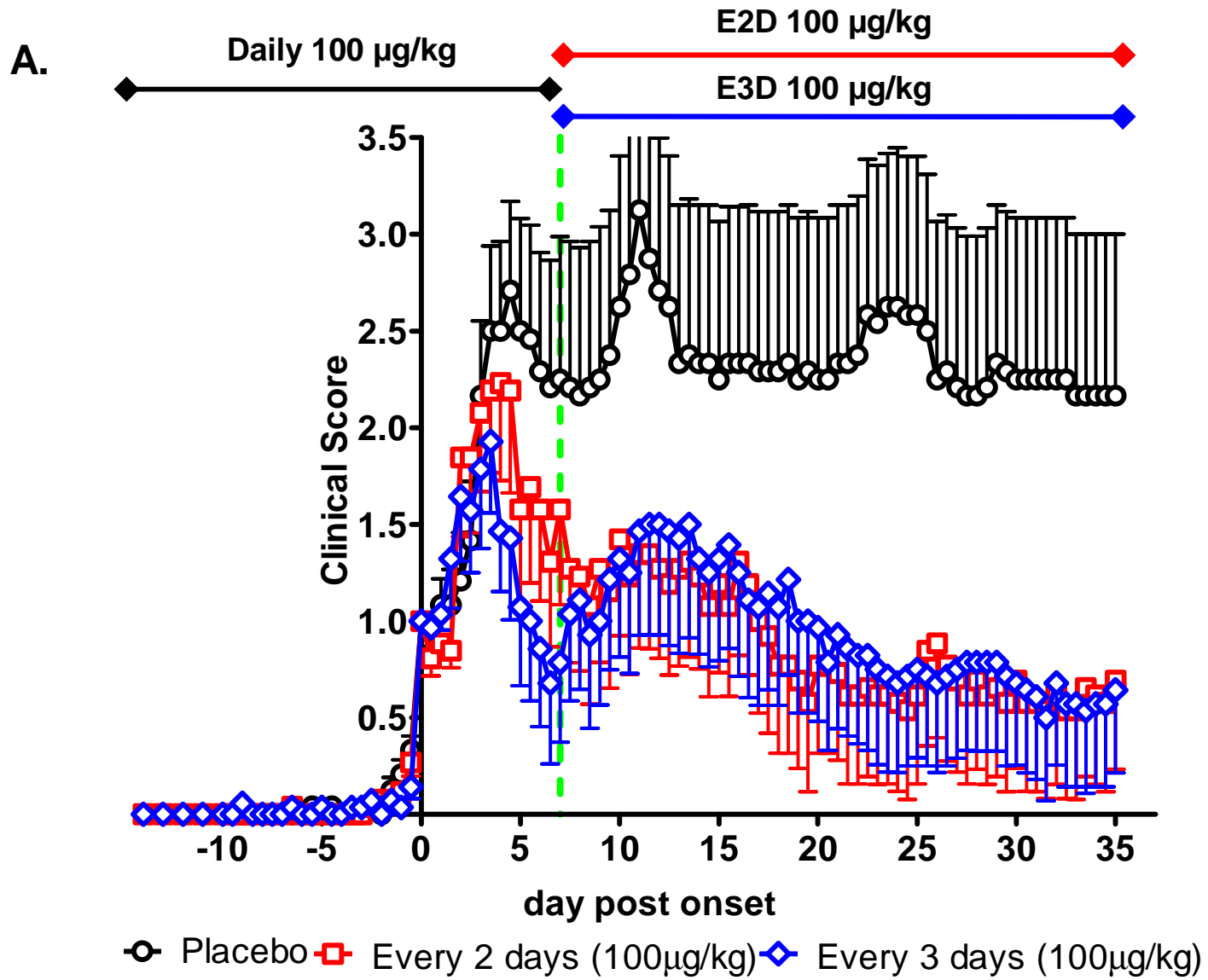| Species	Dose	N	T_{max}(min)	$t_{1/2}$	C_{max}	$AUC_{0\text{-inf\_obs}}$	Cl
Cyno	35	10	5	22.7	23.0	771.9	46.0
	100	14	5	24.5	55.6	2298.4	43.6
	150	16	5	16.7	94.2	2555.9	58.7
	250	2	15	22.8	117.0	5943.2	42.1
	300	5	5	73.5	168.0	8588.5	35.1
	500	2	15	30.8	321.0	17750.6	28.2
	1000	2	15	25.4	852.5	53389.9	18.7
SD Rat	50	6	1	6.1	11.8	102.5	486.6
	150	6	5	10.4	11.6	243.9	617.9
	250	3	5	7.5	36.4	480.5	522.1
	500	9	15	16.4	33.9	1039.6	488.5
	1000	3	5	8.7	53.9	1219.2	819.9

FIGURE 1
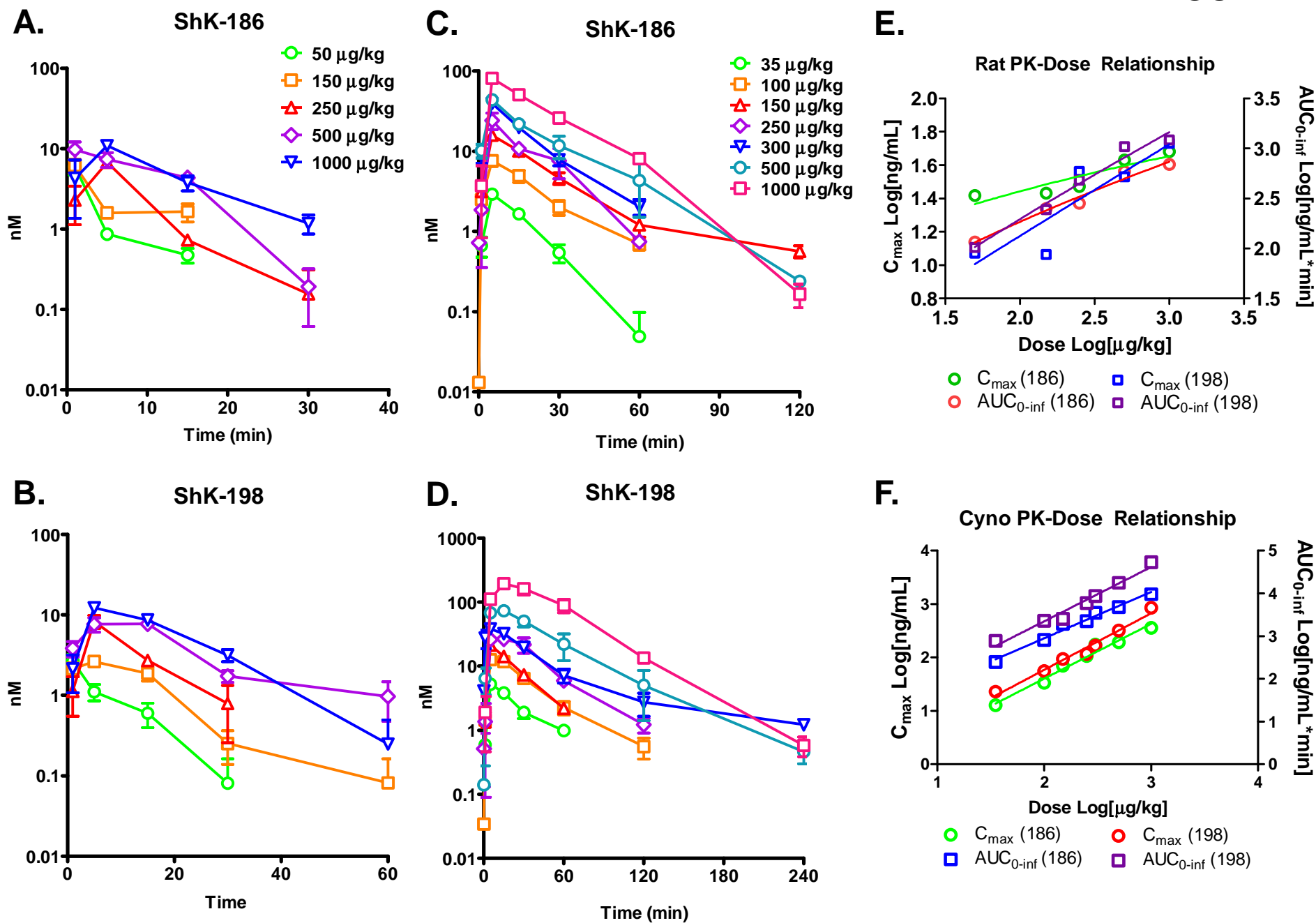
FIGURE 2
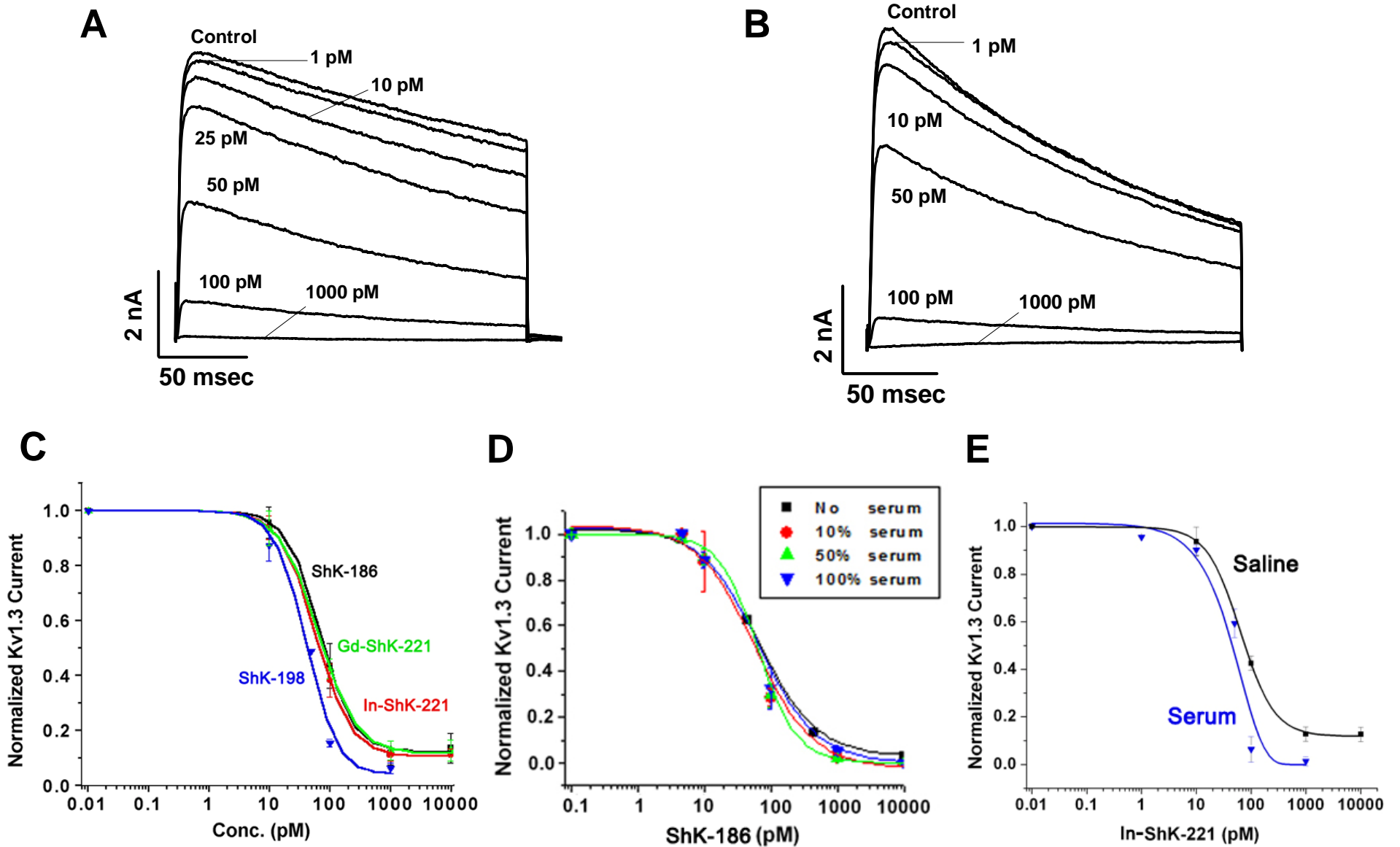
FIGURE 3
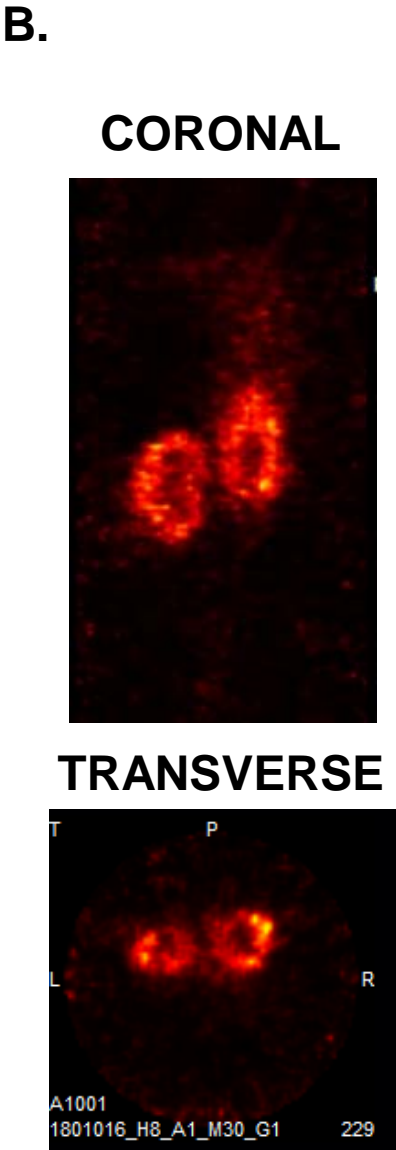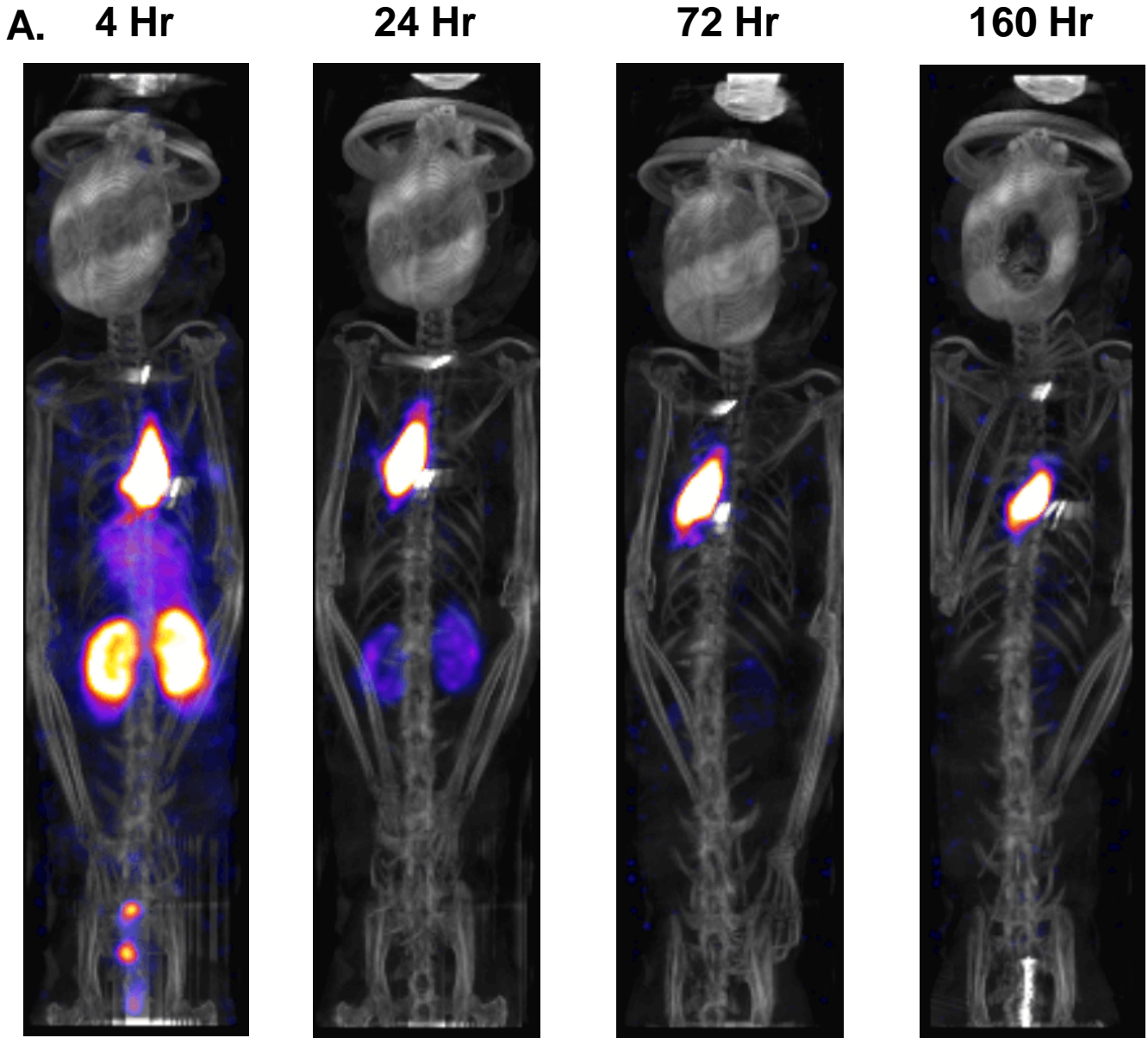
A.

4 Hr	24 Hr	72 Hr	160 Hr

B.

CORONAL

TRANSVERSE
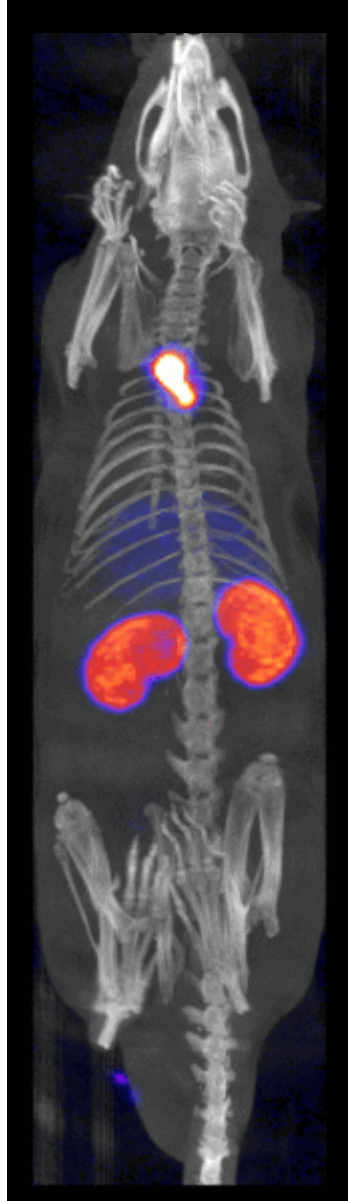
C. 1 Hr   8 Hr   24 Hr
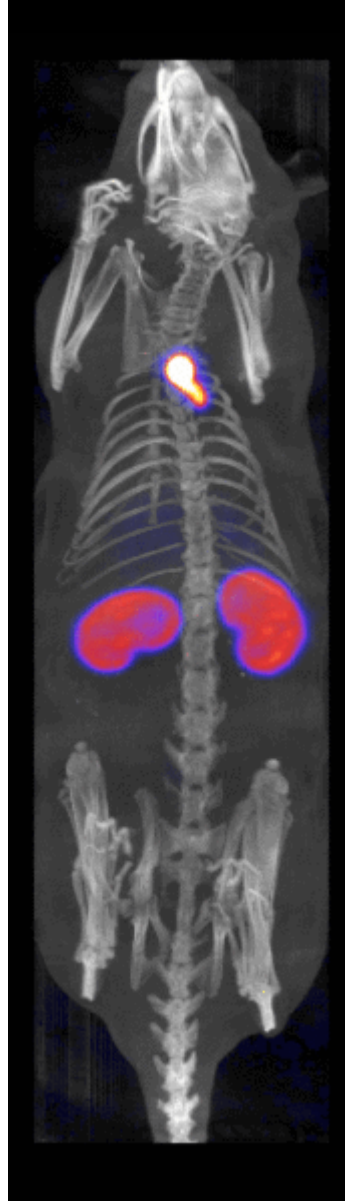
D.   FIGURE 3

CORONAL

TRANSVERSE

A1002
1801016_H4_A1_M30_G2   156

FIGURE 3

E. **Injection Site**

F. **Whole Blood**

FIGURE 4

IL-2 Secretion

FIGURE 5

A.

B.

FIGURE 6

FIGURE 6

Daily or E3D (100µg/kg)

B.

Daily Placebo (P6N)   Daily (100 µg/kg)   Every 3 Days (100 µg/kg)

FIGURE 6

FIGURE 7